Novel design of a planar flow-through potentiometric sensor

Guagneli, Luca; Mousavi, Zekra; Sokalski, Tomasz; Leito, Ivo; Bobacka, Johan

Published in:
Journal of Electroanalytical Chemistry

DOI:
10.1016/j.jelechem.2022.116785

Published: 13/09/2022

Document Version
Final published version

Novel design of a planar flow-through potentiometric sensor

Guagneli, Luca; Mousavi, Zekra; Sokalski, Tomasz; Leito, Ivo; Bobacka, Johan

Published in:
Journal of Electroanalytical Chemistry

DOI:
https://doi.org/10.1016/j.jelechem.2022.116785

Published: 13/09/2022

Document Version
Final published version

Journal of Electroanalytical Chemistry 923 (2022) 116785

Contents lists available at ScienceDirect

Journal of Electroanalytical Chemistry

journal homepage: www.elsevier.com/locate/jelechem

Novel design of a planar flow-through potentiometric sensor

Luca Guagneli [a], Zekra Mousavi [a], Tomasz Sokalski [a], Ivo Leito [b], Johan Bobacka [a,*]

[a] Åbo Akademi University, Johan Gadolin Process Chemistry Centre, Laboratory of Molecular Science and Engineering, Henriksgatan 2, FI-20500 Turku-□bo, Finland
[b] Institute of Chemistry, University of Tartu, Ravila 14a, 50411 Tartu, Estonia

ARTICLE INFO

Keywords:
Potentiometric sensor
Solid-contact
Planar electrode
Potassium ion-selective electrode
Flow-through design

ABSTRACT

A novel planar electrode for flow-through potentiometric sensing is presented in this work. Planar and concentric potassium solid-contact ion-selective electrodes (K^+-SCISEs) were designed and studied using potentiometry and electrochemical impedance spectroscopy (EIS). The K^+-SCISE consisted of a neutral carrier PVC-based ion-selective membrane with valinomycin as ionophore, carbon cloth as ion-to-electron transducer, and a gold wire as electronic conductor, all incased in a polycarbonate support. The prepared electrodes showed a stable and reproducible potentiometric response. The average slopes for three identical flow-through K^+-SCISEs, calibrated once per day during five days (n = 15), was 57.2 mV/decade (SD = 0.9 mV/decade). The corresponding standard potential of the electrodes during five days (n = 15) was 417 mV (SD = 3.6 mV). The water-layer test showed that the ion-selective membrane/carbon cloth interface was not subject to the formation of a water layer. The electrodes had selectivity coefficients comparable to the values obtained from the literature. The resistance of the ion-selective membrane, determined by EIS, was in the range of 45–250 MΩ for the planar electrode geometries studied in this work.

1. Introduction

Ion-selective electrodes (ISEs) are an important group of chemical sensors that allow the determination of more than 50 analytes [1,2]. During the last decades, solid-contact ion-selective electrodes (SCISEs) have gained importance due to their robustness and the possibility of miniaturization and versatile engineering [3–5].

The measurement of electrolyte concentrations in biological samples by ISEs is part of routine medical analysis [6]. Furthermore, non-invasive wearable sensors for health monitoring are becoming an important field of application of SCISEs [7]. Among biological fluids, sweat is easily accessible, especially during physical exercise, and therefore an attractive sample for non-invasive chemical analysis. Such analysis gives important information about several clinically relevant biomarkers. The analytes measured in sweat include electrolytes and pH, metabolites such as glucose and lactate, uric and ascorbic acid, etc. [8,9]. The quantity of electrolytes present in sweat can be linked to some health problems and can be used as a diagnostic tool for e.g. cystic fibrosis [10]. The importance of real-time values of electrolyte concentrations, is leading research towards wearable sensors for sweat-monitoring [9].

The potentiometric sensors used in wearable devices must be robust and able to measure small sample volumes. These requirements create a need to optimize the electrode design. Currently, the most common approaches for wearable potentiometric devices rely on planar geometries [5,9]. Some examples of wearable devices are wristbands [11], watches [12,13], adhesive patches [14–16], tattoos [17–19], textiles [20], and bandages [21]. However, there are some challenges related to wearable chemical sensors that still need to be addressed. These include the mixing of old and new sweat, which can lead to averaged values instead of real-time continuous values [22]. Furthermore, the direct contact of the sensor membrane with the skin surface may restrict sample flow and may cause skin irritation.

Flow-through electrochemical cells [23,24] are sensing platforms that allow continuous monitoring of analytes. Planar electrodes, which are designed to let the sample solution flow through a small opening in the sensing membrane, would allow continuous sample flow without any additional microfluidic conduits. Such an approach should be feasible for wearable on-body sensing applications.

This study presents a new electrode design that combines the properties of a planar SCISE with the advantages of a flow-through measuring cell with sample volumes of a few microliters. Due to its clinical importance, potassium was chosen as the main ion in this proof-of-concept study. The geometry of the ISE was designed to allow the combination of different electrodes in a sandwich-shaped sensing platform,

* Corresponding author.
E-mail address: johan.bobacka@abo.fi (J. Bobacka).

https://doi.org/10.1016/j.jelechem.2022.116785
Received 29 May 2022; Received in revised form 31 August 2022; Accepted 2 September 2022
Available online 13 September 2022

and to minimize the direct contact between the sensing membrane and the skin.

2. Experimental

2.1. Chemicals and materials

Sodium chloride was purchased from VWR. Magnesium chloride hexahydrate and potassium chloride were purchased from Merck. Calcium chloride dihydrate was purchased from Fluka Chemicals. Lithium chloride, lithium acetate (LiOAc, 98%), Iron (III) chloride hexahydrate (>98%), potassium ionophore I (valinomycin), potassium tetrakis [3,5-*bis*(*trifluoromethyl*)-*phenyl*]borate (KTFPB), bis(2-ethylhexyl)sebacate (DOS, ≥97%), high molecular weight polyvinyl chloride (PVC), and tetrahydrofuran (THF, ≥99.5%) were obtained from Sigma-Aldrich. Deionized water (ELGA Purelab Ultra, resistance 18.2 MΩcm) was used for preparing the aqueous solutions. Carbon cloth (Kynol® activated carbon fabric ACC-5092–20) was purchased from Kynol Europa GmbH, Hamburg (Germany). Gold wire (24 carats, diameter 1 mm) was purchased from City Gold, Turku (Finland). Polycarbonate sheet was purchased from ETRA Oy (Finland).

2.2. Design of the planar flow-through K^+-SCISE

The design principle of the planar flow-through SCISE, in comparison with the commonly used design, is illustrated in Fig. 1.

The composition of the potassium ion-selective membrane (K^+-ISM) in % (w/w) was: 1.0 valinomycin, 0.5 KTFPB, 65.2 DOS, and 33.3 PVC. These components were dissolved in THF to obtain a cocktail with 20% dry mass. The cocktail was vigorously shaken for a few minutes, mixed overnight, and then stored in the refrigerator. The ISM was applied using the drop-casting method, as illustrated in Fig. 2.

In this work, carbon cloth (CC) was used as solid-contact material. Carbon cloth is a flexible material, easy to cut and shape with good electrical properties and high specific surface area enabling good ion-to-electron transduction properties [25].

A piece of carbon cloth with the dimensions of ≈ 35 × 35 mm was used. A round hole with a 4 mm diameter was cut in the middle of the carbon cloth. The carbon cloth piece was fixed on a clean PTFE sheet. A 50 μL portion of the K^+-ISM cocktail was drop-cast in the area around the hole (Fig. 2a). This was done to ensure that the CC threads around the hole would stay attached to the cloth. After 45 min, air was blown in the middle of the hole to remove all the remaining loose CC threads. Then a sequence of additions of 4 × 50 μL was made into the hole (Fig. 2b). Each addition was followed by 45 min of drying time. After the fourth addition, the membrane was left to dry for 4 h. Subsequently, the CC piece was turned upside-down and the PTFE support was cleaned. One last addition of 50 μL was made on the bottom side of the membrane, ensuring that the cocktail spreads towards the carbon cloth (Fig. 2c). This last addition was performed to ensure that the K^+-ISM would completely cover the CC also on the bottom side (Fig. 3a). The membranes were left to dry overnight at room temperature.

It was important that the membrane covered the top and bottom surfaces of carbon cloth in order to obtain a tight seal between the membrane and the polycarbonate support in the region of the channel, as illustrated in Fig. 3b. In this work, the measured thickness of the bare carbon cloth was ca 0.3 mm and the total thickness in the area where the membrane covered the carbon cloth was ca 0.4 mm. The membrane thickness in the center of the membrane was ca 0.3 mm.

A hole of 2.5 mm diameter was punched in the middle of the membrane. The CC piece with the K^+-ISM was then sandwiched between two pieces of polycarbonate (PC) support (Fig. 3b). A gold wire was used as electrical contact. One side of the wire was flattened and inserted in the support to be in contact with the CC substrate. The two pieces of polycarbonate support were kept together using screws (Fig. 4). The K^+-ISM acted both as the sensing membrane and as a seal between the K^+-ISM and the polycarbonate support in the region of the sample channel. Three identical K^+-SCISEs (E1, E2, and E3) were prepared and characterized.

2.3. Electrochemical impedance spectroscopy (EIS)

EIS measurements were performed using the Autolab General Purpose Electrochemical System with Autolab Frequency Response Analyzer (FRA) (AUT20.FRA2-Autolab, Eco Chemie, B.V., The Netherlands). The measurements were performed in deaerated 0.1 M KCl solution. A glassy carbon rod and Ag/AgCl/3 M KCl (6.0733.100 Metrohm, Switzerland) were used as the counter and reference electrode, respectively. The impedance spectra were recorded at open-circuit potential in the frequency range 100 kHz–10 mHz by using an ac excitation amplitude of 100 mV.

2.4. Potentiometric measurements

The potentiometric measurements for three identical K^+-SCISEs (E1, E2, and E3) were performed using a 16-channel millivoltmeter (Lawson Labs EMF16 Interface system) with a high input impedance (10^{15} Ω) and L-EMF DAQ 3.0 software. A commercial double-junction Ag/AgCl/3 M KCl reference electrode (6.0726.100 Metrohm, Switzer-

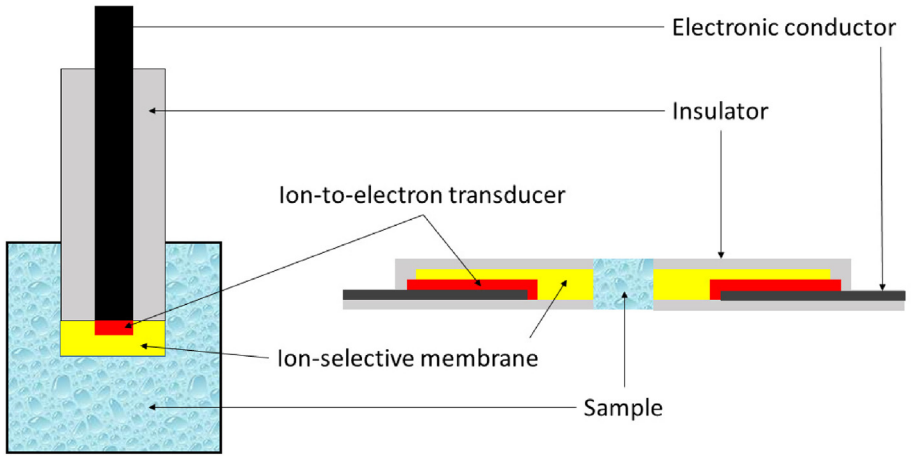

Fig. 1. Schematic representation of a traditional SCISE (*left*) and a planar flow-through SCISE (*right*).

Fig. 2. Schematic representation of the drop-casting process used to cast the K^+-ISM. a) 50 µL addition around the hole, b) 4×50 µL additions in the middle of the hole, c) 50 µL addition on the opposite side of the membrane after turning around the CC piece.

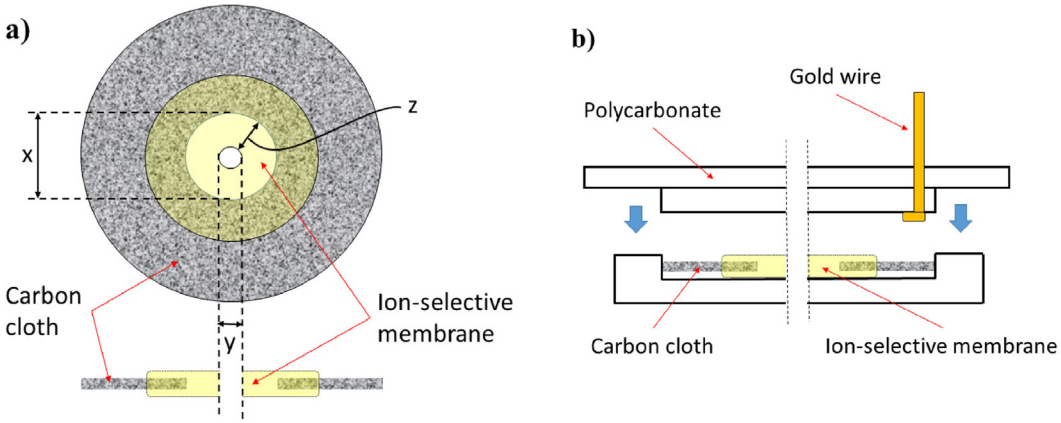

Fig. 3. Illustration of the planar flow-through K^+-SCISE using carbon cloth as ion-to-electron transducer (a) and the polycarbonate support with a gold contact (b). The figure is not drawn to scale.

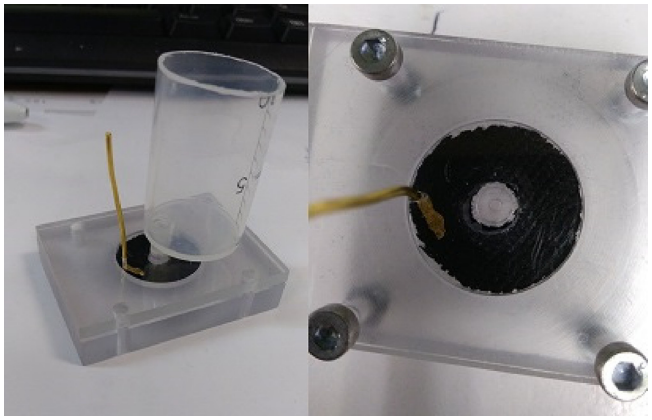

Fig. 4. The setup of the measuring cell with the K^+-SCISE.

land) with 1 M lithium acetate (LiOAc) as outer bridge solution was used. Ion activities were calculated using the extended Debye-Hückel equation.

The potential of the planar K^+-SCISE was measured in 1 M to 10^{-8} M KCl solutions for ca. 5 min at each concentration. The potential was measured every 2 s. The averages of the last five potential values were used to construct the calibration curves.

The water layer test was done by measuring the potential of the planar K^+-SCISE, which was conditioned in 0.1 M KCl for 24 h before starting the test, in 0.1 M KCl solution for 1.5 h, then in 0.1 M NaCl for 2 h, and finally in 0.1 M KCl for 4 h.

The selectivity coefficients (K_{ij}) of the K^+-SCISEs were determined for common interfering cations (Na^+, Ca^{2+}, Mg^{2+}, Li^+) by the separate solution method (SSM) in 0.01 M chloride solutions of the cations.

3. Results and discussion

The planar K^+-SCISE is designed so that it can be combined with a solid-state reference electrode and used in the flow-through mode. However, this work is limited to the characterization of the planar flow-through indicator electrode (K^+-SCISE), as a proof-of-concept. For this purpose, a small container was connected to the upper hole of the polycarbonate support (Fig. 4). The container was filled with sample solution and housed the reference electrode during measurements. The lower hole of the polycarbonate support was closed during measurements. The K^+-SCISEs were stored dry when not in use.

3.1. Electrochemical impedance spectroscopy (EIS)

Impedance measurements were done to study the effect of the geometry of the K^+-ISM, which is determined by the diameter of the hole in CC (x), the diameter of the hole in the K^+-ISM (y) and the resulting membrane width (z) of the K^+-ISM, as shown in Fig. 3a. Results from impedance measurements are shown in Fig. 5. The shape of the impedance spectra of the planar flow-through K^+-SCISE is comparable to that of an ideal SCISE. The high-frequency semicircle is attributed to the bulk resistance of the PVC-based K^+-ISM. The low-frequency impedance curve is due to the ion-to-electron transduction process. As can be seen in Fig. 5a, the resistance of an electrode with

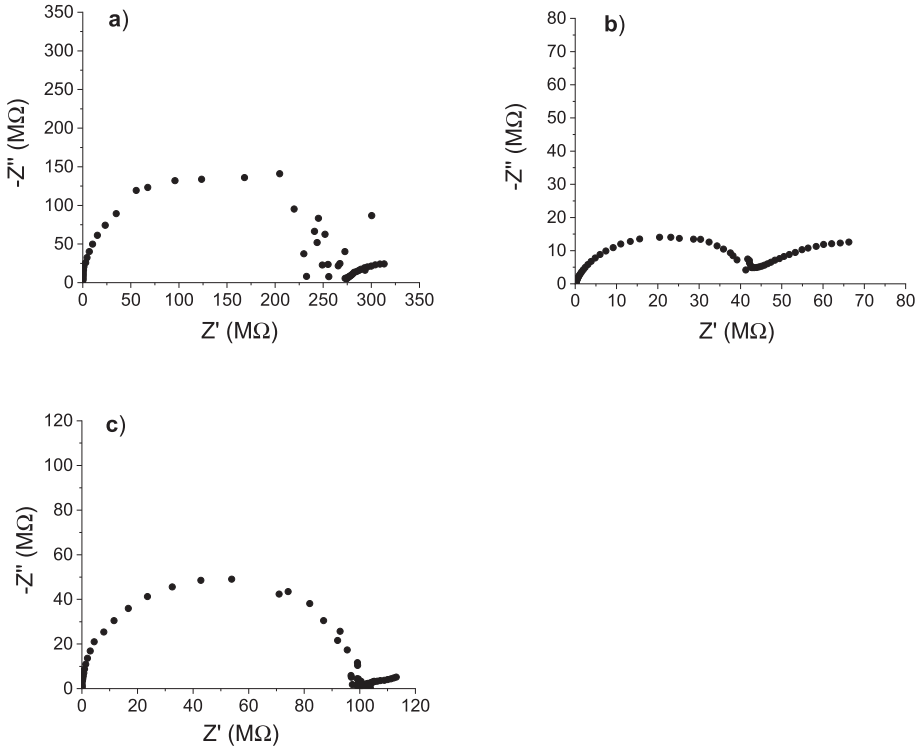

Fig. 5. Examples of EIS spectra of planar flow-through K^+-SCISEs with different geometries (as shown in Fig. 3). a) x = 5 mm, y = 3 mm, z = 1 mm, b) x = 4 mm, y = 3 mm, z = 0.5 mm, c) x = 4 mm, y = 2.5 mm, z = 0.75 mm. The impedance spectra were recorded at open-circuit potential in 0.1 M KCl solution in the frequency range 100 kHz–10 mHz by using an ac excitation amplitude of 100 mV.

x = 5 mm, y = 3 mm, and z = 1 mm is ca. 250 MΩ. By changing the dimensions of the electrode to x = 4 mm, y = 3 mm, and z = 0.5 mm, the resistance of the membrane decreased to ca. 45 MΩ (Fig. 5b). However, this configuration was not optimal from the fluidistics point of view. Since the hole in the membrane (3 mm) was slightly bigger than that in the channel (2.5 mm), the result was a recessed membrane in the channel where solution was easily trapped. To overcome this problem, the dimensions were ultimately changed to x = 4 mm, y = 2.5 mm, and z = 0.75 mm. As shown in Fig. 5c, the electrode in this case had a resistance of ca. 100 MΩ, which is satisfactory from the resistance point of view and which resolved the technical problem of the recessed membrane.

This latter geometry (x = 4 mm, y = 2.5 mm, z = 0.75 mm) was used in the rest of the experiments presented here. Although the resistance of the membranes was relatively high (ca 100 MΩ), the potentiometric response of the cell was highly satisfactory.

3.2. Calibration curves and potential stability

The potential of the cell, consisting of a planar flow-through K^+-SCISE (E1) as the indicator electrode and a Metrohm double junction reference electrode, was measured in 1 M to 10^{-8} M KCl solutions (Fig. 6a). The test was done without and with 0.1 M NaCl as constant background electrolyte (BGE).

As shown in Fig. 6a, the device gives a linear response over a wide KCl concentration range (1 M – 10^{-5} M KCl). As the concentration of potassium ions in sweat is generally in the order of 2–8 mmol/L [26,27], the range of potassium ion concentrations chosen for further characterization was 10^{-1} M to 10^{-4} M. Fig. 6b shows a representative calibration curve for E1 with and without 0.1 M NaCl as BGE in this concentration range.

The average slopes for three K^+-SCISEs (E1-E3) were 57.3 ± 0.6 and 56.3 ± 0.4 mV/decade (average ± SD, n = 3) in calibrations done without and with 0.1 M NaCl as BGE, respectively.

The performance of the novel K^+-SCISE is comparable to or better than those studied earlier in sweat-monitoring devices using valinomycin as ionophore. Pirovano et al. presented a wearable potentiometric system based on solid-contact ISEs to measure the concentration of K^+ in sweat [12]. The authors reported slopes of 45.7 ± 7.4 mV/decade in the linear activity range (10^{-4}–$10^{-0.5}$) when using poly(3,4-ethylenedioxythiophene) (PEDOT) as solid contact, and slopes of 54.3 ± 1.5 mV/decade in the linear activity range (10^{-4}–10^{-1}) when using poly(3-octylthiophene) (POT) as the solid contact [12]. Also Alizadeh et al. presented a wearable patch used to determine K^+ in sweat [15]. The authors reported a sensitivity of ~53.9 mV/decade for potassium ions. Parrilla et al. presented a textile-based stretchable wearable sensor for monitoring K^+ ions in sweat [20], which showed a linear response in the activity range 10^{-5}–10^{-1} with a slope of 59.9 mV/decade. In another study, Parrilla et al. presented a wearable patch for monitoring K^+ ions in sweat, which showed a slope of 56.8 ± 2.5 mV/decade for K^+ in the activity range 10^{-5}–10^{-1} [16]. The linearity and sensitivity (slope) of the novel K^+-SCISE studied in this work is thus well in accordance with other electrodes intended for the same purpose.

In order to study the reproducibility of the electrode response, the potential of the K^+-SCISE was measured in KCl solutions starting from low to high concentration and then back to low concentration (Fig. 7).

As can be seen in Fig. 7a, the potentiometric response of the sensor is reproducible. The electrode has a high signal stability over a timeframe of minutes and the time for achieving stable potential was less than 1–2 min.

The day-to-day stability of the calibration plot is important for wearable applications to minimize the need for recalibration. For this reason, the potentiometric performance of three identical K^+-SCISEs (E1, E2, and E3) was measured during five consecutive days. The test was performed by calibrating the electrodes in 10^{-1} M to 10^{-4} M KCl solutions with 0.1 M NaCl as BGE. The results are shown in Table 1.

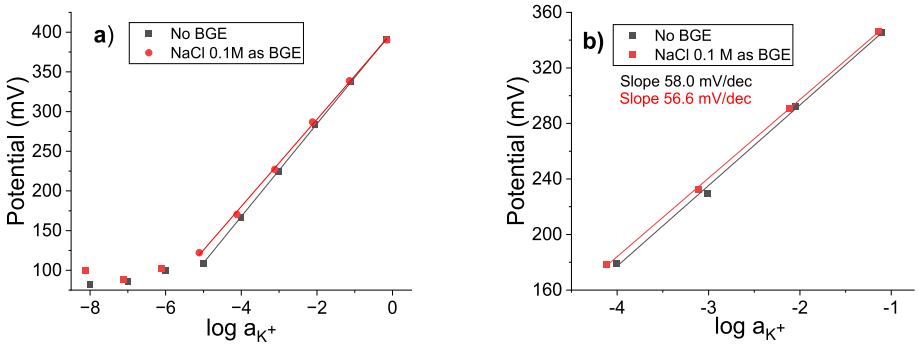

Fig. 6. a) The calibration curve of a planar flow-through K^+-SCISE recorded in 1 M to 10^{-8} M KCl solutions without (black), and with (red) 0.1 M NaCl as BGE. b) Comparison between calibration curves for a K^+-SCISEs obtained in KCl solutions without (black) and with (red) 0.1 M NaCl as BGE.

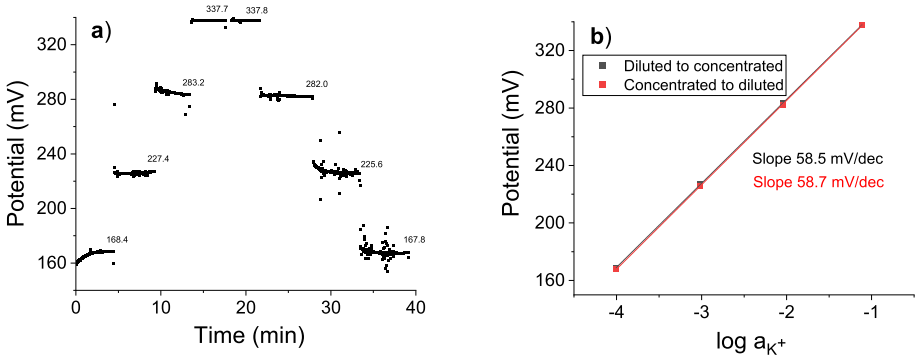

Fig. 7. a) The potential-time response obtained by measuring the potential of the electrode in KCl solutions starting from low to high concentration and then back to low concentration, b) calibration curves obtained using the final potential values from a).

Table 1
Inter-day calibrations of K^+-SCISEs measured in 10^{-1} M to 10^{-4} M KCl solutions with 0.1 M NaCl as BGE for five consecutive days.

Day	Slope (mV/decade)			Standard potential (mV)		
	E1	E2	E3	E1	E2	E3
1	56.9	58.2	59.6	415	414	420
2	57.0	55.6	56.8	417	415	423
3	57.0	57.1	57.2	418	420	424
4	56.2	57.2	57.5	414	421	423
5	56.5	57.4	58.0	417	420	424

During five days, the change in the slopes of E1, E2, and E3 was within the ranges of 0.8, 2.6, and 2.8 mV/decade, respectively. The average slopes for the three identical flow-through K^+-SCISEs (E1, E2, E3) during five days (n = 3 × 5 = 15), was 57.2 mV/decade (SD = 0.9 mV/decade). The corresponding average standard potential of the electrodes during five days (n = 15) was 417 mV (SD = 3.6 mV).

3.3. Water layer test

The water layer test proposed by Fibbioli et al. aims to identify the presence of a water layer between the ISM and the solid contact [28]. The test is performed after complete conditioning of the ISM in a solution of the primary ion. First, the potential is measured in the solution of the primary ion. Then the potential is measured in a solution containing an interfering ion. Finally, the potential is measured again in the solution of primary ion.

The presence of an aqueous layer causes a positive potential drift when changing the sample solution from the primary cation to a solution with an interfering cation. In addition, when changing the sample solution from the interfering cation to the primary cation solution a negative potential drift indicates the existence of an aqueous layer.

The results from the water-layer test for three K^+-SCISEs (E1, E2, and E3) are shown in Fig. 8. A significant potential drift is observed when the electrodes are in contact with the interfering ion solution (0.1 M NaCl). The extent of the drift is different for the electrodes E1, E2, and E3. However, no potential drift is observed when changing from interfering to primary ion solution. From these results, it can be concluded that the presence of a water layer is very unlikely. The observed drifts in 0.1 M NaCl can tentatively be related to leaching of K^+ ions from the K^+-ISM into the small sample volume in the flow-through cell.

3.4. Selectivity coefficients

The K^+-SCISE presented in this work is intended for sweat monitoring. Therefore, the most relevant interfering cations are Na^+, Ca^{2+}, Li^+, and Mg^{2+}. The selectivity measurement was carried out for three

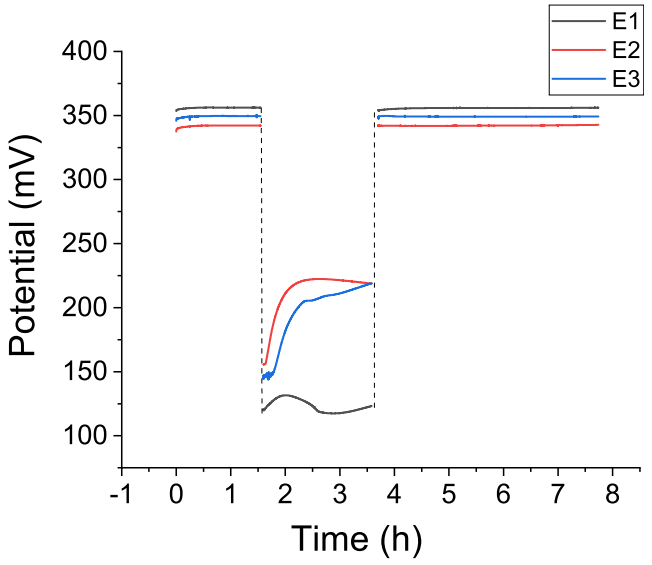

Fig. 8. Results from the water layer test performed by measuring the potential first in 0.1 M KCl, then in 0.1 M NaCl and finally in 0.1 M KCl solutions using E1 (black), E2 (red), and E3 (blue) electrodes.

Table 2
Selectivity coefficients for three K^+-SCISEs ± standard deviation (SD) between electrodes.

$logK_{i,j}$	Ca^{2+}	Li^+	Mg^{2+}	Na^+
Average ± SD	−4.29 ± 0.14	−3.21 ± 0.09	−4.68 ± 0.05	−3.34 ± 0.08

Table 3
Comparison of selectivity coefficients measured in this study with those reported in the literature.

	This study[a]	[16][a]	[29][b]	[30][a]
$\log K_{K,Ca}$	−4.3 ± 0.1	−3.7 ± 0.1	−3.9 ± 0.1	−4.7 ±0.1
$\log K_{K,Li}$	−3.2 ± 0.1	−3.5 ± 0.0	−2.7 ± 0.1	−4.4 ± 0.1
$\log K_{K,Mg}$	−4.7 ± 0.1	−3.9 ± 0.0	−4.1 ± 0.1	−4.9 ± 0.2
$\log K_{K,Na}$	−3.3 ± 0.1	−3.7 ± 0.0	−2.8 ± 0.1	−3.2 ± 0.2

[a] Separate solution method (SSM).
[b] Fixed interference method (FIM).

K^+-SCISEs (E1, E2, and E3) using the separate solution method (SSM). Results in Table 2 show the average values of the selectivity coefficients, as log $K_{i,j}$, measured for three electrodes ± the standard deviation (SD), while Table 3 below shows a comparison of the selectivity coefficient values obtained in this study with those of K^+-SCISEs presented in the literature. It can be concluded that the planar flow-through K^+-SCISE presented in this study shows selectivity coefficients that are in line with other K^+-selective electrodes presented in the literature.

4. Conclusions

A new design of a planar flow-through ion-selective electrode was introduced in this work. The proof-of-concept was provided for a potassium-selective solid-contact electrode (K^+-SCISE) utilizing carbon cloth as ion-to-electron transducer and a plasticized PVC-based ion-selective membrane with valinomycin as ionophore. The analytical performance of the suggested electrode design was evaluated by potentiometry and electrochemical impedance spectroscopy. The average potentiometric slopes for three identical flow-through K^+-SCISEs, calibrated once per day during five days (n = 15), was 57.2 mV/decade (standard deviation = 0.9 mV/decade). The corresponding standard potential of three electrodes during five days (n = 15) was 417 mV (standard deviation = 3.6 mV). The observed analytical performance shows that the suggested electrode design is feasible. The K^+-SCISEs used in this work were prepared by manual drop-casting, hole-cutting, and mechanical assembly into a polycarbonate support. However, the suggested design should be compatible with automated manufacturing via e.g. printing technologies.

The planar flow-through design presented here is expected to have several advantages compared to existing designs. First, the planar electrode contains a relatively high amount of ion-selective membrane material and a large contact area with the solid contact material, which ensures high robustness and potential stability. Second, thanks to the concentric design, the contact area between the electrode and the sample is very small, enabling a small sample volume. Third, when considering applications such as wearable on-body sensing of sweat, the ion-selective membrane will not be in direct contact with skin, thus avoiding skin irritation. Fourth, the sweat sample can freely flow through the sensor, thus ensuring sample renewal during continuous measurements.

In this work, the emphasis was on the fabrication and characterization of the indicator electrode but we hope that the same design can be used also for a solid-state reference electrode. The suggested design should enable a multi-sensor approach by stacking a multi-layer structure with several indicator electrodes and a reference electrode with a small sample channel running through the device.

CRediT authorship contribution statement

Luca Guagneli: Formal analysis, Investigation, Writing – original draft. **Zekra Mousavi:** Investigation, Writing – review & editing, Supervision. **Tomasz Sokalski:** Investigation, Writing – review & editing, Supervision. **Ivo Leito:** Writing – review & editing, Supervision. **Johan Bobacka:** Conceptualization, Methodology, Writing – review & editing, Supervision, Project administration.

Data availability

Data will be made available on request.

Declaration of Competing Interest

The authors declare that they have no known competing financial interests or personal relationships that could have appeared to influence the work reported in this paper.

Acknowledgements

Luca Guagneli gratefully acknowledges the support from the EU via the Excellence in Analytical Chemistry (EACH) Erasmus Mundus programme (Grant Agreement No 2017-1937/001-002).

References

[1] P. Bühlmann, E. Pretsch, E. Bakker, Carrier-based ion-selective electrodes and bulk optodes. 2. Ionophores for potentiometric and optical sensors, Chem. Rev. 98 (1998) 1593–1688, https://doi.org/10.1021/cr970113+.
[2] K.N. Mikhelson, Ion-selective electrodes, Springer (2013), https://doi.org/10.1007/978-3-642-36886-8.
[3] J. Bobacka, A. Ivaska, A. Lewenstam, Potentiometric ion sensors, Chem. Rev. 108 (2008) 329–351, https://doi.org/10.1021/cr068100w.
[4] A. Michalska, All-solid-state ion-selective and all-solid-state reference electrodes, Electroanalysis 24 (2012) 1253–1265, https://doi.org/10.1002/elan.201200059.
[5] Y. Shao, Y. Ying, J. Ping, Recent advances in solid-contact ion-selective electrodes: functional materials, transduction mechanisms, and development trends, Chem. Soc. Rev. 49 (2020) 4405–4465, https://doi.org/10.1039/C9CS00587K.

[6] A. Lewenstam, M. Maj-Zurawska, A. Hulanicki, Application of ion-selective electrodes in clinical analysis, Electroanalysis 3 (1991) 727–734, https://doi.org/10.1002/elan.1140030802.
[7] Y. Lyu, S. Gan, Y. Bao, L. Zhong, J. Xu, W. Wang, Z. Liu, Y. Ma, G. Yang, L. Niu, Solid-contact ion-selective electrodes: Response mechanisms, transducer materials and wearable sensors, Membranes 10 (2020) 128, https://doi.org/10.3390/membranes10060128.
[8] W. Gao, G.A. Brooks, D.C. Klonoff, Wearable physiological systems and technologies for metabolic monitoring, J. Appl. Physiol. 124 (2018) 548–556, https://doi.org/10.1152/japplphysiol.00407.2017.
[9] M. Bariya, H.Y.Y. Nyein, A. Javey, Wearable sweat sensors, Nat. Electron. 1 (2018) 160–171, https://doi.org/10.1038/s41928-018-0043-y.
[10] A. Lynch, D. Diamond, M. Leader, Point-of-need diagnosis of cystic fibrosis using a potentiometric ion-selective electrode array, Analyst 125 (2000) 2264–2267, https://doi.org/10.1039/b006379g.
[11] W. Gao, S. Emaminejad, H.Y.Y. Nyein, S. Challa, K. Chen, A. Peck, H.M. Fahad, H. Ota, H. Shiraki, D. Kiriya, D.-H. Lien, G.A. Brooks, R.W. Davis, A. Javey, Fully integrated wearable sensor arrays for multiplexed in situ perspiration analysis, Nature 529 (2016) 509–514, https://doi.org/10.1038/nature16521.
[12] P. Pirovano, M. Dorrian, A. Shinde, A. Donohoe, A.J. Brady, N.M. Moyna, G. Wallace, D. Diamond, M. McCaul, A wearable sensor for the detection of sodium and potassium in human sweat during exercise, Talanta 219 (2020), https://doi.org/10.1016/j.talanta.2020.121145 121145.
[13] T. Glennon, C. O'Quigley, M. McCaul, G. Matzeu, S. Beirne, G.G. Wallace, F. Stroiescu, N. O'Mahoney, P. White, D. Diamond, 'SWEATCH': A wearable platform for harvesting and analysing sweat sodium content, Electroanalysis 28 (2016) 1283–1289, https://doi.org/10.1002/elan.201600106.
[14] D.P. Rose, M.E. Ratterman, D.K. Griffin, L. Hou, N. Kelley-Loughnane, R.R. Naik, J. A. Hagen, I. Papautsky, J.C. Heikenfeld, Adhesive RFID sensor patch for monitoring of sweat electrolytes, IEEE Trans. Biomed. Eng. 62 (2015) 1457–1465, https://doi.org/10.1109/TBME.2014.2369991.
[15] A. Alizadeh, A. Burns, R. Lenigk, R. Gettings, J. Ashe, A. Porter, M. McCaul, R. Barrett, D. Diamond, P. White, P. Skeath, M. Tomczak, A wearable patch for continuous monitoring of sweat electrolytes during exertion, Lab. Chip 18 (2018) 2632–2641, https://doi.org/10.1039/C8LC00510A.
[16] M. Parrilla, I. Ortiz-Gómez, R. Cánovas, A. Salinas-Castillo, M. Cuartero, G.A. Crespo, Wearable potentiometric ion patch for on-body electrolyte monitoring in sweat: Toward a validation strategy to ensure physiological relevance, Anal. Chem. 91 (2019) 8644–8651, https://doi.org/10.1021/acs.analchem.9b02126.
[17] T. Guinovart, A.J. Bandodkar, J.R. Windmiller, F.J. Andrade, J. Wang, A potentiometric tattoo sensor for monitoring ammonium in sweat, Analyst 138 (2013) 7031–7038, https://doi.org/10.1039/C3AN01672B.
[18] A.J. Bandodkar, V.W.S. Hung, W. Jia, G. Valdés-Ramírez, J.R. Windmiller, A.G. Martinez, J. Ramírez, G. Chan, K. Kerman, J. Wang, Tattoo-based potentiometric ion-selective sensors for epidermal pH monitoring, Analyst 138 (2013) 123–128, https://doi.org/10.1039/C2AN36422K.
[19] A.J. Bandodkar, W. Jia, J. Wang, Tattoo-based wearable electrochemical devices: A review, Electroanalysis 27 (2015) 562–572, https://doi.org/10.1002/elan.201400537.
[20] M. Parrilla, R. Cánovas, I. Jeerapan, F.J. Andrade, J. Wang, A textile-based stretchable multi-ion potentiometric sensor, Adv. Healthc. Mater. 5 (2016) 996–1001, https://doi.org/10.1002/adhm.201600092.
[21] T. Guinovart, G. Valdés-Ramírez, J.R. Windmiller, F.J. Andrade, J. Wang, Bandage-based wearable potentiometric sensor for monitoring wound pH, Electroanalysis 26 (2014) 1345–1353, https://doi.org/10.1002/elan.201300558.
[22] J. Heikenfeld, Non-invasive analyte access and sensing through eccrine sweat: Challenges and outlook circa 2016, Electroanalysis 28 (2016) 1242–1249, https://doi.org/10.1002/elan.201600018.
[23] S. Böhm, W. Olthuis, P. Bergveld, A generic design of a flow-through potentiometric sensor array, Microchim. Acta 134 (2000) 237–243, https://doi.org/10.1007/s006040070043.
[24] S. Alegret, J. Alonso, J. Bartroli, J.L.F.C. Lima, A.A.S.C. Machado, J.M. Paulis, Flow-through sandwich PVC matrix membrane electrode for flow injection analysis, Anal. Lett. 18 (1985) 2291–2303, https://doi.org/10.1080/00032718508068619.
[25] U. Mattinen, S. Rabiej, A. Lewenstam, J. Bobacka, Impedance study of the ion-to-electron transduction process for carbon cloth as solid-contact material in potentiometric ion sensors, Electrochim. Acta 56 (2011) 10683–10687, https://doi.org/10.1016/j.electacta.2011.07.082.
[26] S.J. Montain, S.N. Cheuvront, H.C. Lukaski, Sweat mineral-element responses during 7 h of exercise-heat stress, Int. J. Sport Nutr. Exerc. Metab. 17 (2007) 574–582, https://doi.org/10.1123/ijsnem.17.6.574.
[27] I.L. Schwartz, J.H. Thaysen, Excretion of sodium and potassium in human sweat, J. Clin. Invest. 35 (1956) 114–120, https://doi.org/10.1172/JCI103245.
[28] M. Fibbioli, W.E. Morf, M. Badertscher, N.F. de Rooij, E. Pretsch, Potential drifts of solid-contacted ion-selective electrodes due to zero-current ion fluxes through the sensor membrane, Electroanalysis 12 (2000) 1286–1292, https://doi.org/10.1002/1521-4109(200011)12:16<1286::AID-ELAN1286>3.0.CO;2-Q.
[29] M. Novell, M. Parrilla, G.A. Crespo, F.X. Rius, F.J. Andrade, Paper-based ion-selective potentiometric sensors, Anal. Chem. 84 (2012) 4695–4702, https://doi.org/10.1021/ac202979j.
[30] J. Zhu, X. Li, Y. Qin, Y. Zhang, Single-piece solid-contact ion-selective electrodes with polymer–carbon nanotube composites, Sens. Actuators B:Chem. 148 (2010) 166–172, https://doi.org/10.1016/j.snb.2010.04.041.